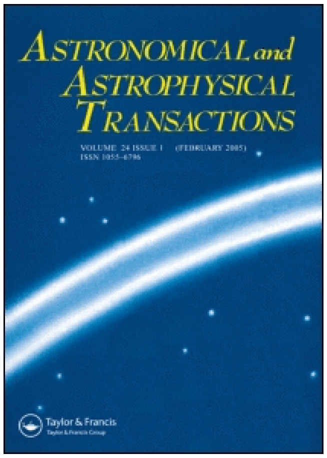

Astronomical & Astrophysical Transactions
The Journal of the Eurasian Astronomical Society
Publication details, including instructions for authors and subscription information:
http://www.informaworld.com/smpp/title~content=t713453505

On the anomalous balmer decrement in the orion nebula

S. Gulyaev; S. Pyatkes; R. L. Sorochenko; E. Chentzov

Online Publication Date: 01 January 1995
To cite this Article: Gulyaev, S., Pyatkes, S., Sorochenko, R. L. and Chentzov, E. (1995) 'On the anomalous balmer decrement in the orion nebula', Astronomical & Astrophysical Transactions, 6:3, 197 - 211
To link to this article: DOI: 10.1080/10556799508232067
URL: http://dx.doi.org/10.1080/10556799508232067

Astronomical and Astrophysical Transactions, 1995,
Vol. 6, pp. 197–211
Reprints available directly from the publisher.
Photocopying permitted by license only

ON THE ANOMALOUS BALMER DECREMENT IN THE ORION NEBULA

S. GULYAEV[1], S. PYATKES[1], R. L. SOROCHENKO[2], and E. CHENTZOV[3]

[1] *ul. Lenina 51, Ekaterinburg 620083, Russia*
[2] *Leninskij prosp. 53, 117924 Moscow, Russia*
[3] *Nizhy Arkhyz, Zelenchukskij region, Stavropolsky Territory, 357147 Russia*

(Received August 10, 1993)

New measurements of Balmer lines in the central part of the Orion nebula have been made on the 6-m telescope. The generalized curve of the level population is compiled from the Balmer line and radio line measurements. A new approach to the problem of the anomalous Balmer decrement is proposed. The relative level populations obtained from our relative intensity measurements are referred to the theoretical population curve in the range of high principal quantum numbers n = 20–30. It provides matching of our populations with the level populations derived from radio recombination line observations and from high-n Balmer line measurements by Goad *et al.* (1972). However, the low-n level population proves to be much lower than the theoretical ones. When interpreting the results of the observations, the inhomogeneity of the population structure of the low-l states is taken into account. The radiative transitions $nd \rightarrow 2p$ is shown to play the main role in the Balmer line emission. Absorption from the metastable level $2s$ also can be important in the Balmer line radiation transfer. We show that the anomalously low intensity of the low-n Balmer lines cannot be explained only with the use of the effect of optical depth. It is possible that the anomaly in the low-n Balmer line intensities is caused by the real underpopulation of the nd-states when $n < 15$.

KEY WORDS Orion nebula, Balmer decrement, radio recombination lines, atomic level population

1 INTRODUCTION

Almost 30 years, since the work of Kaler (1966), the problem of anomalous Balmer decrement in the spectrum of the Orion nebula attracts attention of astrophysicists. One usually formulates this problem as follows: in the Orion nebula and in several other nebulae the intensities of Balmer lines (relative to the intensity of Hβ), arising from levels with a high principal quantum number n, were systematically much greater than could be accounted for by recombination theories.

Several attempts, both theoretical and observational, were made to explain this anomaly, but unsuccessfully.

So, Kaler (1968) has attempted to explain these differences by supposing that electron temperatures in the nebulae were lower than previously expected. But for the Orion nebula, this explanation is untenable, since it leads to temperature estimates of less than 1500 K.

Miller (1971) suggested that a part of the difficulty may be a systematic error in the spectrophotographic intensity measurements. But the reliability of the spectrophotographic data was confirmed later in the observational work of Goad *et al.* (1972) and by our new careful observations reported in this paper.

It seemed that the Lyman pumping mechanism proposed by Beigman *et al.* (1980) and Hoang–Binh (1983) allowed to produce the overpopulation of high levels and, hence, to explain the anomalous Balmer decrement in the Orion nebula spectrum. This mechanism is based on the suggestion that, in the stars of the spectral type later than O5, the Lyman line emission at $\lambda > 912$ Å can be significantly higher than the intensity of the UV continuum at $\lambda < 912$ Å which ionizes the HII region.† In the framework of this suggestion, the situation was considered where the ionization rate by Lyman continuum photons can become less than, or of the order of, the excitation rate by the Lyman line radiation. As a result, large Lyman discontinuity in the stellar flux would increase the departure coefficients b_n at $n < 50$ well above the values occurring in HII regions excited by hotter stars. Under some circumstances, the departure coefficients b_n for $n \leq 50$ could even exceed 1.

To investigate this prediction, some observational studies of radio recombination lines (RRLs) have been made. Sorochenko *et al.* (1988) have analyzed the results of the RRL for the Orion nebula. They considered lines in the range from H 39α to H 110α and found that experimental b_n-values are in a good agreement with calculations of Salem and Brocklehurst (1979) and contradict the calculations performed with allowance for the role of the Lyman discontinuity in the exciting star spectrum. Also, the millimeter-wave recombination lines show no significant indication of excitation by Lyman line radiation from a nearby exciting star (Hoang–Binh *et al.*, 1985; Gordon and Walmsley, 1990). Thus, the observations of RRLs testify to the absence of the additional Lyman pumping mechanism.

Gulyaev and Zavlin (1994) proposed an explanation to the observational fact of the absence of the Lyman pumping mechanism in real nebulae. The idea was that, when calculating the stellar spectrum in the vicinity of the Lyman discontinuity, the effect of lowering of the atomic ionization potential in the plasma microfield should be taken into account. To allow for this effect, they used the so-called non-realization model developed by Gundel (1970, 1971), Sevastyanenko (1985), Hummer and Mihalas (1988), Gulyaev (1988), etc. The inclusion of this effect into stellar atmosphere calculations reduces the Lyman discontinuity substantially, so that the ratio of the Lyman line absorption to radiative recombination drives towards the blackbody values, and thereby the effect of the additional Lyman pumping mechanism is cancelled.

Thus, the Lyman pumping mechanism, which seemed to explain the anomaly of the Balmer decrement in the spectrum of the Orion nebula, now appears to be

†The Lyman discontinuity cannot be observed directly because of UV extinction in the HII region, in the interstellar matter, and in the terrestrial atmosphere.

disproven both observationally and theoretically. This brings back the old problem of the anomalous Balmer decrement in the Orion nebula.

In this paper we report new observations of the Balmer decrement in the Orion nebula, performed with the stellar spectrograph of the 6-m telescope. We propose a new approach to the problem of the Balmer decrement. So far, all attempts to explain the differences between observation and theory were based on an anomalously high intensity of high-n Balmer lines. But relative measurements do not allow to determine what is really abnormal – either the intensity of the high-n lines is anomalously high, as it is suggested since Kaler's work, or, on the contrary, the intensity of the low-n lines is anomalously low. In view of the absence of the Lyman pumping mechanism, the latter interpretation of the relative measurements is developed in this paper. We obtain relative level populations, and match them to theoretical populations of high-n levels (n = 20–30) and to the data on radio recombination lines. Consequently, the derived populations of low-n levels prove to be much lower than the theoretical ones.

The paper is divided into five parts. In Section 2 we discuss some details of observational techniques and the data reduction applied. Section 3 deals with the equations which determine the emission and absorption coefficients and with the equations of transfer. We deduce expressions for the weighted departure coefficients which can be found from the Balmer line intensity measurements. In Section 4 we present results of our observations in a form of the generalized atomic level population curve and discuss some possible reasons of anomalously low intensity of the low-n Balmer lines (population of low-n levels). Summarizing remarks are given in Section 5.

2 OBSERVATIONS

The intensity measurements were obtained from high-dispersion spectra of the Orion nebula taken with the stellar spectrograph of the 6-m telescope, with a dispersion of 14 and 7 Å mm^{-1}. All the spectra were taken on baked IIaO plates. The observations were made with a long slit (about 15 arcsec) with a south–north orientation, at a point near the Trapezium with the coordinates $\alpha = 5^h32^m48^s$, $\delta = -5°25'30''$ (Jan 1984) and $\alpha = 5^h34^m38^s$, $\delta = -5°23'30''$ (Dec 1987). The observation parameters are listed in Table 1.

To minimize errors, all the stages of the observations, measurements, data processing, and corrections were performed very carefully.

With the use of prisms, the spectrum was widened after the first 60 minutes of exposure. Due to this method, two spectra with essentially different exposures were obtained on one plate. This has allowed us to exclude errors connected with the procedure of matching weak and strong lines of the nebula spectrum.

The microdensitometer tracing of the nebula spectra were first measured to find the level of the underlying continuum at the Balmer series limit. This was initially done by hand; later an automatic system "SPECTRUM" (Nazarenko, 1990) was

Table 1. Observation Parameters

Date	*Exposure (minutes)*	*Dispersion (Å mm^{-1})*	*Spectral Range (Å)*	*Observer*
1984 January 14	155	14	3400–5000	Chentzov
1987 December 2	195	7	3000–4100	Chentzov

used to check this extrapolation. The difference between the two results was found to be negligible.

The correction has been made for the variation of the atmospheric extinction with wavelength and zenith distance (during the long time of exposure). With this purpose, the spectra of the standard star ζ Ori were taken before and after the exposure.

To transform the densities of the plate into intensities, we used the spectrum of Sirius (α CMa), obtained right in this set of observations. The relative intensities of the non-overlapping Balmer lines ($7 \leq n \leq 29$) and of the remaining partially resolved lines were found with a Gaussian fitting program.

Hβ is a model-dependent spectral line. The effect of optical depth must be taken into account for a theoretical interpretation of this line (Pottash, 1960). Density inhomogeneities and velocity fields in the nebula complicate the situation very much. In addition, when measuring the intensities of weak high-n Balmer lines relative to the strong Hβ one, there inevitably appear the problems of the calibration of photographic plates, the matching of the photographic and photoelectric data, and some other problems, which promote a growth of errors. To avoid the uncertainty and minimize errors, we used the H21-line instead of Hβ. An optically thin line of moderate intensity, H21 is more convenient for this purpose.[†]

The derived intensities of the lines have been corrected for reddening. But due to the two reasons – the narrowness of the spectral interval and the adopted procedure of normalization (H21=100) – the largest applied correction was no more than several percent.

The possible systematic errors in the values of relative line intensities are small. For the resolved lines over the wavelength region from H7 to H29, they are expected to be less than 5 percent. For the higher Balmer series lines ($n \geq 30$) the error increases with n fast, approaching 20–50 percent.

The observed relative intensities of Balmer lines relative to the intensity of H21 are presented in Figure 1. The results of our measurements are shown by crosses. The data of Kaler (1966), being renormalized in the same way, are shown in Figure 1 by squares (photographic) and by asterisks (photoelectric data).

The reduced observational data allow to investigate the atomic population structure. In the next section we will consider the elementary theory of the emission and absorption coefficients and the radiation transfer problem in Balmer lines. This will

[†]Goad *et al.* (1972) measured relative intensities of Balmer series relative to the intensity of the first 10 Å of the Balmer continuum.

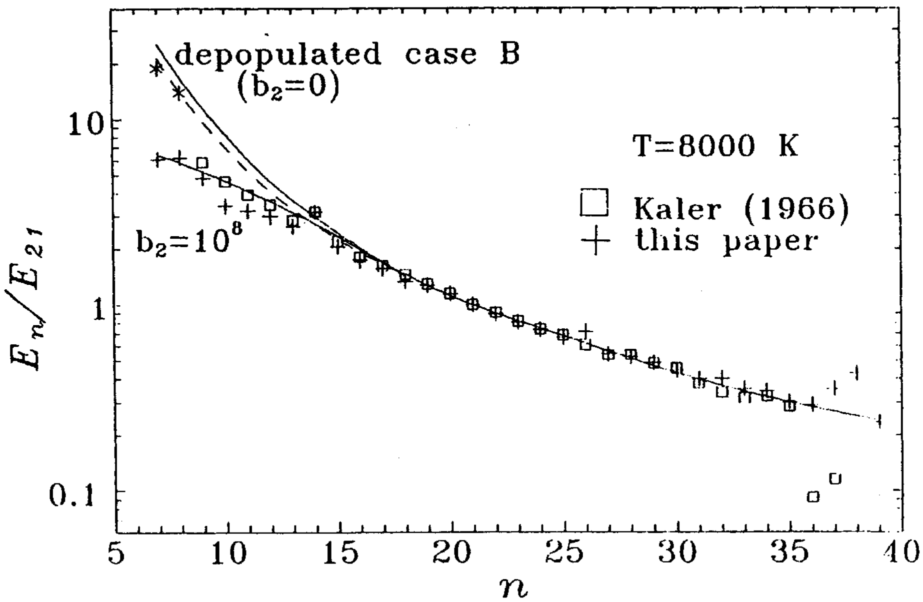

Figure 1 The observed Balmer line intensity relation E_n/E_{21} for the Orion Nebula. Crosses – our observations; squares and asterisks – Kaler (1966). Solid lines – the computed values for T_e = 8000 K, $N_e = 10^4$ cm^{-3}; dashed line – the same for T_e = 8000 K, $N_e = 10^5$ cm^{-3}. The calculations are indicated for the depopulated Case B (b_2 = 0) and for the hypothetical case of optically thick Balmer lines (see Section 4).

help us to specify the level population characteristics, which can be found from the relative intensity measurements.

3 THEORY OF THE BALMER DECREMENT

3.1 Emission and Absorption Coefficients

The frequency of the transition between an upper level n and a lower level n' of hydrogen is given by the Rydberg formula,

$$\nu = Rc\left(\frac{1}{n'^2} - \frac{1}{n^2}\right), \tag{1}$$

where R is the Rydberg constant.

A spectral line emission is a product of the line components formed by radiative transitions between degenerate quantum states nl of the upper level and $n'l'$ of the lower level. The line emission coefficient at frequency ν' can be written as

$$j_L = \frac{h\nu}{4\pi}\sum_{ll'} b_{nl}N^*_{nl}A_{nln'l'}\phi_{nln'l'}(\nu'), \tag{2}$$

where summation over the angular-momentum states l and l' is controlled by the selection rules, $\phi_{nln'l'}(\nu)$ is the normalized profile function

$$\int_{-\infty}^{\infty} \phi_{nln'l'}(\nu') = 1; \tag{3}$$

further we will assume $\phi_{nln'l'}(\nu')$ to be the same for all the transitions $nl \rightarrow n'l'$, that is $\phi_{nln'l'}(\nu') \equiv \phi_{nn'}(\nu')$. The appropriate rate of the spontaneous radiative transition A is given by

$$A_{nln'l'} = \frac{64\pi^4 e^2}{3hc^3}\nu^3 |r_{nln'l'}|^2 \frac{\max(l,l')}{(2l+1)}, \tag{4}$$

where r is the coordinate matrix element. In (2), the departure coefficients b_{nl} are defined as N_{nl}/N^*_{nl}, where N_{nl} is the population of the nl-th state, and N^*_{nl} is the population computed for local thermodynamic equilibrium (LTE) using the Saha equation.

Eq. (2) can be expressed in terms of weighted values

$$j_L = \frac{h\nu}{4\pi}\langle b_n\rangle_{n'} N^*_n A_{nn'}\phi_n(\nu'). \tag{5}$$

The weighted A is

$$A_{nn'} = \sum_{ll'} A_{nln'l'}\omega_{nl}/\omega_n, \tag{6}$$

where ω_{nl} is the statistical weight of the nl-state, and $\omega_n = \sum_l \omega_{nl}$. The LTE population of the level n is $N^*_n = \sum_l N^*_{nl}$; it is connected with the nl-state LTE population by

$$\frac{N^*_n}{\omega_n} = \frac{N^*_{nl}}{\omega_{nl}}. \tag{7}$$

The weighted $\langle b_n\rangle_{n'}$, in (5) is given by

$$\langle b_n\rangle_{n'} = \frac{\sum_{ll'} \omega_{nl} b_{nl} A_{nln'l'}}{\sum_{ll'} \omega_{nl} A_{nln'l'}} = \frac{\sum_{ll'} \omega_{nl} b_{nl} A_{nln'l'}}{\omega_n A_{nn'}}. \tag{8}$$

Using eq. (4), one can rewrite (8) as

$$\langle b_n\rangle_{n'} = \frac{\sum_{ll'} \max(l,l') b_{nl} |r_{nln'l'}|^2}{\sum_{ll'} \max(l,l') |r_{nln'l'}|^2}. \tag{9}$$

In the case of a radio recombination line H$n\alpha$ (transition $n+1 \rightarrow n$), summations in eqs. (8) and (9) are extended over all nl-states. For a Balmer line ($n \rightarrow 2$) there remain only three components in the sums – ns, np and nd; thus, eq. (8) becomes

$$\langle b_n\rangle_2 = \frac{b_{ns}A_{ns2p} + 3b_{np}A_{np2s} + 5b_{nd}A_{nd2p}}{A_{ns2p} + 3A_{np2s} + 5A_{nd2p}}, \tag{10}$$

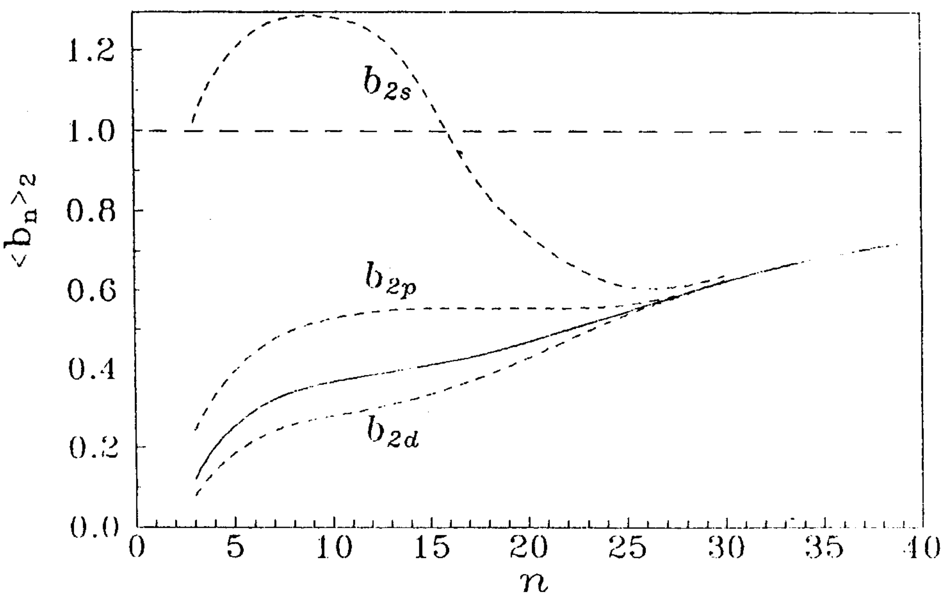

Figure 2 The hydrogen population structure. Case B – depopulated $n = 2$ levels. $N_e = 10^4$ cm^{-3} and $T_e = 10^4$ K. Dashed lines – variation of b_{ns}, b_{np} and b_{nd} with n calculated by Summers (1977). Solid line – $\langle b_n \rangle_2$ as a function of n.

whence, using expressions for the radial matrix elements (Bethe and Salpeter, 1957), we get

$$\langle b_n \rangle_2 = \frac{b_{ns}a_s + b_{np}a_p + b_{nd}a_d}{a_s + a_p + a_d}, \tag{11}$$

where $a_s = 1$, $a_p = 12(n^2 - 1)/n^2$, and $a_d = 32(n^2 - 1)/(n^2 - 2)$. When $n \gg 1$, the following approximation is valid:

$$\langle b_n \rangle_2 \approx (1/45)(b_{ns} + 12b_{np} + 32b_{nd}). \tag{12}$$

It is clear that the weights of the np- and nd-states in eq. (12) are much larger than the weight of the ns-state.

The general behavior of the excited-state population structure was calculated by several authors (Brocklehurst, 1971; Summers, 1977; Hummer and Storey, 1987). The curves b_{ns}, b_{np} and b_{nd} as functions of n are shown in Figure 2 with dashed lines. They were computed for Case B, $N_e = 10^4$ cm^{-3} and $T_e = 10^4$ K (Summers, 1977). With the use of eq. (10), we have calculated the weighted $\langle b_n \rangle_2$ (solid line in Figure 2).

It is the weighted quantity $\langle b_n \rangle_2$ that one can obtain from the spectral line intensity measurements.

The line absorption coefficient at frequency ν' can be written as

$$k_L = \frac{h\nu}{4\pi}\phi_{nn'}(\nu')\sum_{ll'}(b_{n'l'}N^*_{n'l'}B_{n'l'nl} - b_{nl}N^*_{nl}B_{nln'l'}). \tag{13}$$

Here $B_{nln'l'}$ and $B_{n'l'nl}$ are the Einstein B-coefficients for induced emission and absorption:

$$B_{n'l'nl} = \frac{c^2}{2h\nu^3}A_{nln'l'} \tag{14}$$

and

$$B_{n'l'nl} = \frac{\omega_n}{\omega_{n'}}B_{nln'l'} \tag{15}$$

Substituting (14) and (15) and taking into account (7) and (6), eq. (13) becomes

$$k_L = \frac{h\nu}{4\pi}\phi_n(\nu')(\langle b_{n'}\rangle_n N^*_{n'}B_{n'n} - \langle b_n\rangle_{n'}N^*_n B_{nn'}), \tag{16}$$

where

$$\langle b_{n'}\rangle_n = \frac{\sum\limits_{ll'}\omega_{nl}b_{n'l'}A_{nln'l'}}{\omega_n A_{nn'}}, \tag{17}$$

and the Einstein coefficients $B_{nn'}$, $B_{n'n}$ and $A_{nn'}$ are connected with each other by analogy with (14) and (15).

It is convenient to express the relation between the true emission and absorption coefficients and their equilibrium values as

$$j_L = \langle b_n\rangle_{n'}\, j^*_L \tag{18}$$

and

$$k_L = \langle b_{n'}\rangle_n \left[\frac{1-(\langle b_n\rangle_{n'}/\langle b_{n'}\rangle_n)\exp(-h\nu/kT_e)}{1-\exp(-h\nu/kT_e)}\right]k^*_L. \tag{19}$$

In case of transitions $n \longrightarrow 2$ (Balmer series lines),

$$j_L = \langle b_n\rangle_2\, j^*_L \tag{20}$$

and

$$k_L = \langle b_2\rangle_n \left[\frac{1-(\langle b_n\rangle_2/\langle b_2\rangle_n)\exp(-h\nu/kT_e)}{1-\exp(-h\nu/kT_e)}\right]k^*_L, \tag{21}$$

where

$$\begin{aligned}\langle b_2\rangle_n &= \frac{b_{2p}a_s + b_{2s}a_p + b_{2p}a_d}{a_s + a_p + a_d} \approx \\ &\approx 0.27b_{2s} + 0.73b_{2p} \approx 0.27b_{2s} \quad (b_{2s} \gg b_{2p}).\end{aligned} \tag{22}$$

When $T \approx 10^4$ K (HII region) and $n \geq 5$, we have $h\nu/kT_e \simeq$ 3–4 and $\langle b_2\rangle_n \gg \langle b_n\rangle_2$, and the following approximation is valid for the Balmer series lines

$$k_L \approx \langle b_2\rangle_n k^*_L. \tag{23}$$

3.2 Radiation Transfer and Line Intensities

The standard equation for the radiation transfer,

$$\frac{dI}{ds} = j - kI, \tag{24}$$

has the following solution:

$$I = \int_0^\tau S \exp(-\tau')\, d\tau' + I_0 \exp(-\tau), \tag{25}$$

so that, assuming homogeneity,

$$I = S[1 - \exp(-\tau')] + I_0 \exp(-\tau). \tag{26}$$

Here τ' and τ are the element of and the total depth through the HII region, I is the intensity of radiation at a given frequency, and I_0 is the radiation originating behind the cloud. S is the source function related to the emission and absorption coefficients by $S = j/k$. Under the LTE conditions, Kirchoff's law holds and S is equal to the Planck function $B(T_e)$. Using this fact, eq. (20) and the definition of the optical depth $\tau = \int k\, ds'$, we then have

$$S = \frac{j}{k} = \frac{j_L + j_C}{k_L + k_C} = B(T_e)\frac{\langle b_n\rangle_{n'}\tau_L^* + \tau_C}{\tau_L + \tau_C}, \tag{27}$$

whence, assuming $I_0 = 0$, eq. (26) becomes

$$I = B(T_e)\frac{\langle b_n\rangle_{n'}\tau_L^* + \tau_C}{\tau_L + \tau_C}[1 - \exp(-(\tau_L + \tau_C))], \tag{28}$$

where the subscript C refers to the continuum.

The "excess" intensity at the line frequency is obtained by subtracting the intensity of the adjacent continuum from eq. (28), thus:

$$I_L = I - I_c = B(T_e)\left[\frac{\langle b_n\rangle_{n'}\tau_L^* + \tau_C}{\tau_L + \tau_C}\left(1 - e^{-(\tau_L + \tau_C)}\right) - \left(1 - e^{-\tau_C}\right)\right]. \tag{29}$$

Assuming $\tau_C \ll \tau_L$, this becomes

$$I_L = B(T_e)\langle b_n\rangle_{n'}\tau_L^*\left(\frac{1 - e^{-\tau_L}}{\tau_L}\right). \tag{30}$$

In the optically thin case ($\tau_C \ll \tau_L \ll 1$) eq. (29) reduces to the usual expression,

$$I_L = B(T_e)\langle b_n\rangle_{n'}\tau_L^*. \tag{31}$$

The total energy emitted in the nn' transition is

$$E_L = \int I_L(\nu')\, d\nu', \tag{32}$$

whence, using eq. (30) and assuming Gaussian shapes for the spectral lines, the relation of the intensities of two Balmer series lines ($n \to 2$ and $m \to 2$) is

$$\frac{E_n}{E_m} = \frac{\langle b_n \rangle_2 N_n^* B_{n2} h\nu_{n2}}{\langle b_m \rangle_2 N_m^* B_{m2} h\nu_{m2}} \frac{f(\tau_{n2})}{f(\tau_{m2})} = \frac{\langle b_n \rangle_2 g_{n2} e^{\chi_n} m^3}{\langle b_m \rangle_2 g_{m2} e^{\chi_m} n^3} \frac{f(\tau_{n2})}{f(\tau_{m2})}, \tag{33}$$

where g_n is the Gaunt factor, τ_{n2} and ν_{n2} are the optical depth and the frequency at the line center, $\chi_n = hRc/n^2kT_e$, and

$$f(a) = \frac{1}{a\sqrt{\pi}} \int_{-\infty}^{\infty} \left[1 - \exp\left(-a \exp\left(-x^2\right)\right)\right] dx. \tag{34}$$

The function $f(a)$ can be expanded into a series as

$$f(a) = \sum_{k=0}^{\infty} (-1)^k \frac{a^k}{(k+1)!\sqrt{k+1}}; \tag{35}$$

$f \approx 1$ in the optically thin case ($\tau_L + \tau_C \ll 1$).

Thus, assuming homogeneity, the relation of the weighted departure coefficients of the two levels n and m can be found from the measurements of the relative intensities E_n/E_m of the Balmer lines Hn and Hm using the following expression:

$$\frac{\langle b_n \rangle_2}{\langle b_m \rangle_2} = \frac{E_n}{E_m} \frac{n^3 e^{-\chi_n}}{m^3 e^{-\chi_m}} \frac{g_{m2} f(\tau_{m2})}{g_{n2} f(\tau_{n2})}. \tag{36}$$

Using eq. (36) and other formulae of this section, we have analyzed our observational data.

4 RESULTS AND DISCUSSION

In Section 2 we have presented our results in the form of the line intensity relation E_n/E_{21} and explained the advantages of using a weak H21 instead of a strong and optically thick Hβ. Under this normalization, the low-n Balmer line relative intensities do not agree with the theoretical curve.

In principle, one cannot determine from relative intensity measurements what is really abnormal – either the intensity of high-n lines is anomalously high, or, on the contrary, it is consistent with the theory, but then the intensity of low-n lines is anomalously low. It is the latter interpretation of the relative measurements that we develop in this paper.

Using eq. (36), and assuming the optically thin case and $T = 8000$ K in the Orion Nebula (Sorochenko *et al.*, 1988), we have calculated the ratio $\langle b_n \rangle_2 / \langle b_{21} \rangle_2$ as a function of n (Figure 3). The variation of the electron density from 10^4 to 10^5 cm^{-3} (solid and dashed lines, respectively) does not affect the theoretical curves

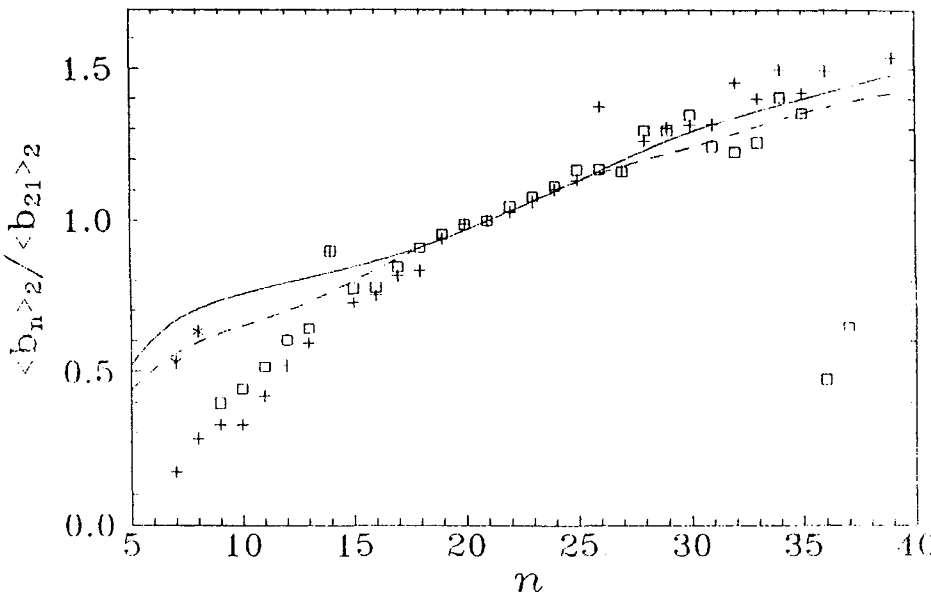

Figure 3 The observed relation $\langle b_n \rangle_2 / \langle b_{21} \rangle_2$ as a function of n. Our data are indicated by crosses, data of Kaler (1966), by squares. Solid line – the computed values for the depopulated Case B, $T = 8000$ K and $N_e = 10^4$ cm^{-3}; dashed line – the same for $N_e = 10^5$ cm^{-3}.

much. The data of Kaler (1966), being renormalized in the same way, are shown with squares. They agree with our data (crosses) almost everywhere. One can see in Figure 3 a similar situation as we met in Figure 1 – since we have normalized all the data to the high-n line, the derived relative populations of low-n levels prove to be much lower than the theoretical ones

Absolute measurements in soft UV (Goad *et al.*, 1972) and in radio wavelengths (RRLs) testify that the high-n level populations in the Orion Nebula agree with the theory.

Goad *et al.* (1972) have found that when $n \geq 15$ not only the *gradient* of the populations is close to its theoretical value, but also the derived *absolute* populations of high levels are in a good agreement with the theory. Unfortunately, they did not consider intensities of the low-n Balmer lines.

RRLs have been observed in the Orion Nebula in a wide spectral range from millimeter-wavelength lines (see, e.g. Wilson and Pauls, 1984; Hoang-Binh *et al.*, 1985; Sorochenko *et al.*, 1988; Gordon, 1989; Gordon and Walmsley, 1990) to meter wavelength RRLs (see Catalogue of RRLs by Gulyaev and Sorochenko (1983)). The radiation transfer, line broadening and maser effect can be taken into account easily when calculating the level populations. The compilation of data made by Sorochenko *et al.* (1988) suggests that the absolute values of the departure coefficients derived from RRL observations ($n \geq 39$) are in a good agreement with the calculated b_n's (e.g., Salem and Brocklehurst, 1979).

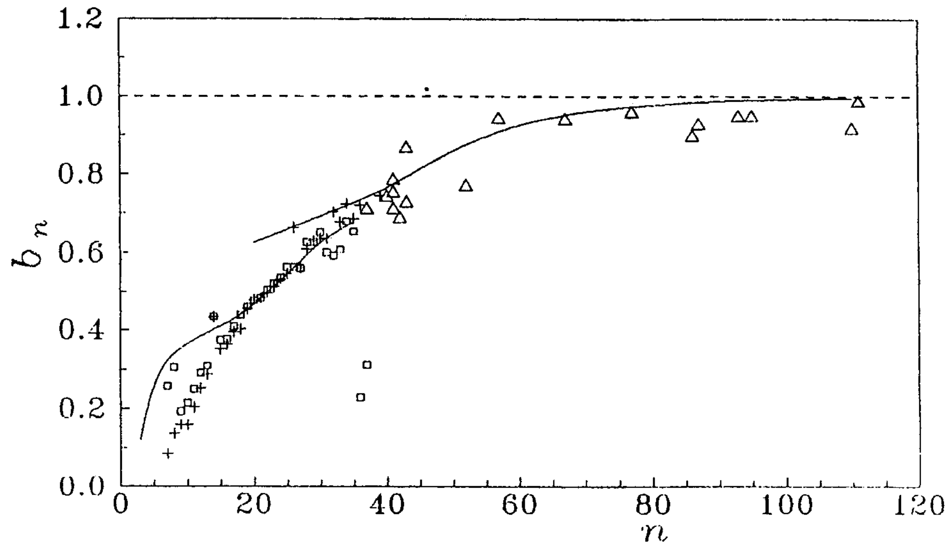

Figure 4 The generalized curve of hydrogen level population in the Orion Nebula. Solid lines – calculations of $\langle b_n \rangle_2$ and b_n for the depopulated Case B, T_e = 8000 K, $N_e = 10^4$ cm^{-3}. The observed departure coefficients are shown by triangles (RRL observations), crosses (our Balmer line measurements) and squares (Kaler's data).

Therefore, the absolute measurements of high-n spectral lines verify the hypothesis adopted in this paper, namely that the problem is not in high-n, but in low-n levels and lines.

Following this hypothesis, we can refer the departure coefficients obtained from the intensity measurements to the theoretical b_n-curve in the range of high n; specifically, at $n = 21$. Consequently, our b_n-values prove to be consistent with the theoretical b_n-curve and with the b_n's obtained from UV (Goad *et al.*, 1972) and radio (RRLs) observations.

In Figure 4 the compilation of all the data available is presented. Two kinds of theoretical curves are shown with solid lines: the weighted $\langle b_n \rangle_2$ calculated for the Balmer series (eq. (11)), and the b_n-values averaged over all nl-states for the RRL observations. Figure 4 shows the b_n-values derived from observations of RRLs (triangles), from our Balmer line measurements (crosses), and from the observations of Kaler (squares). One can see from Figure 4 that there is very good agreement between the theoretical and observed departure coefficients when n is high ($n > 15$). But the difference between theory and observations is essential when n is low.

One possible explanation of the low-n anomaly is that an incorrect approximation was used when going over from line intensities E_n to the departure coefficients b_n. For example, neglecting the optical depth in the low-n Balmer lines could affect the result. We assumed $\tau_{n2} \ll 1$ for all n and put $f(\tau_{n2}) = 1$ in the formulae for E_n (33) and b_n (36).

The idea of a large optical depth of low-n Balmer lines was first proposed by Pottash (1960). On the face of it, this idea seems to be a likely one. The absorption coefficient and the optical depth in a Balmer line depend on the population of the metastable level $2s$ (see eqs. (23) and (22)). According to calculations of Summers (1977), the departure coefficient of this level b_{2s} is very large, changing from approximately 10^6 to 10^8 with the increase of distance from the exciting star. Therefore, the absorption coefficient in a Balmer line proves to be very large because of a strong overpopulation of the metastable level.

Using (22) and (23) and assuming that the profile function is the Gaussian, the absorption coefficient in the center of a Balmer line is given by

$$k_{n2} = 1.8 \times 10^{-13} N_e^2 b_{2s} n^{-3} (1 - 4/n^2)^{-4} g_{n2}, \tag{37}$$

whence the optical depth in the line center is

$$\begin{aligned} \tau_{n2} &= 1.8 \times 10^{-13} \mathrm{EM}\, b_{2s} n^{-3} (1 - 4/n^2)^{-4} g_{n2} \\ &\approx 1.6 \times 10^{-13} \mathrm{EM}\, b_{2s} n^{-3}, \end{aligned} \tag{38}$$

where $\mathrm{EM} = \int N_e^2\, ds$ is the emission measure.

In principle, the agreement between the theoretical curve of intensities and the observational values could be reached by adjusting the product EM b_{2s} in (38). In Figure 1, a hypothetical situation is shown when EM $b_{2s} \approx 10^{16}$ pc cm^{-6}. In this case eq. (38) could be approximated by the expression

$$\tau_{n2} \approx (10/n)^3 (1 - 4/n^2)^{-4}, \tag{39}$$

which gives too high values of the optical depth in the Balmer lines. When n decreases, the optical depth would increase from $\tau \approx 1$ in the center of H10 to $\tau \approx 50$ in the center of Hβ.

For EM $= 10^7$ pc cm^{-6}, which is typical for the central part of the Orion nebula, we would have $b_{2s} \approx 10^9$. The latter value is also unsuitable for it is greater by a factor of several than even the upper limit of b_{2s} in the calculations of Summers (1977).

Therefore, the effect of the optical depth by itself appears to be unable to explain the anomaly of the line intensities. It is possible that other effects are to be taken into account. For example, the intensities of the strongest spectral lines (low-n Balmer lines) can be sensitive to the velocity field structure of the nebula (see, e.g., Spitzer, 1968). Further, one can see from Figure 1 that there is a weak dependence of the Balmer line relative intensities E_n/E_{21} on the plasma electron density. Hence, the electron density influences the departure coefficients derived from observations with the use of the normalization procedure described in this paper. However, too high electron density $N_e > 10^6$ cm^{-3} is required to get the agreement between the observations and theory. Note, that a dense matter with $N_e = 10^5$–10^6 cm^{-3} is actually observed in clumps and knots which are abundant in the central part of the Orion Nebula.

One more possibility should be considered, that Figure 4 gives the actual picture of the atomic level population in the Orion Nebula. Then the low-n hydrogen levels are really underpopulated comparing to the calculations made for the depopulated Case B of Baker and Menzel (1938) and for $N_e = 10^4$ cm^{-3} and $T_e = 8000$ K.

5 CONCLUSIONS

We have reported new spectrophotographic observations of Balmer series lines in the Orion Nebula made with the 6-m telescope. A new approach to the problem of the anomalous Balmer decrement has been proposed. The relative level populations, that we figured out from our relative intensity measurements, were referred to the theoretical population curve in the range of high principal quantum numbers $n = 20$–30. Our data agree well with the level populations derived from radio recombination line observations and from high-n Balmer line measurements of Goad *et al.* (1972). Thus, the generalized population curve in the range of principal quantum numbers from $n = 7$ to $n = 120$ has been obtained. As a result of the procedure proposed, low-level populations ($n < 15$) proved to be much lower than their theoretical values. Some possible reasons of this discrepancy are discussed. We have shown that the explanation based on the idea of self-absorption in the optically thick lines appears to be invalid. Most probably, the real underpopulation of low atomic levels in plasma of the Orion Nebula takes place.

Acknowledgments

We are grateful to the staff of the Special Astrophysical Observatory for making available to us the 6-m telescope for observations. We wish to acknowledge the support of an American Astronomical Society grant. One of us (S. G.) is grateful to Professor M. J. Seaton for bringing the work of Hummer and Storey (1987) to our notice.

References

Baker, J. G. and Menzel, D. H. (1938) *Astrophys. J.* **88**, 52.
Beigman, I. L., Gaisinskiy, I. M., Smirnov, G. T. and Sorochenko, R. L. (1980) *Preprint No. 141 P. N. Lebedev Phys. Inst.* (Moscow).
Bethe, H. A. and Salpeter, E. E. (1957) *Quantum Mechanics of One and Two Electron Atoms* (Berlin-Gottingen-Heidelberg: Springer).
Goad, L. E., Goldberg, L. and Greenstein, J. E. (1972) *Astrophys. J.* **175**, 117.
Gordon, M. (1989) *Astrophys. J.* **337**, 782.
Gordon, M. and Walmsley, C. M. (1990) *Astrophys. J.* **365**, 606.
Gulyaev, S. A. (1988) In T. Nugis and I. Pustil'nik (eds.) *Wolf-Rayet Stars and Related Objects* (Tallin), p. 245.
Gulyaev, S. A. and Sorochenko, R. L. (1983) *Catalogue of Radio Recombination Lines*, Preprints No. 145, 146 and 168, P. N. Lebedev Phys. Inst. (Moscow).
Gulyaev, S. A. and Zavlin, V. E. (1993) *Astron. Astrophys. Trans.* (in press).
Gündel, H. (1970) *Beitr. Plasmaphys.* **10**, 455.
Gündel, H. (1971) *Beitr. Plasmaphys.* **11**, 1.
Hoang-Binh, D. (1983) *Astron. Astrophys.* **121**, L19.

Hoang–Binh, D., Encrenaz, P. and Linke, R. A. (1985) *Astron. Astrophys.* **146**, L19.
Hummer, D. G. and Mihalas, D. (1988) *Astrophys. J.* **331**, 794.
Hummer, D. G. and Storey, P. J. (1987) *Mon. Not. R. Astr. Soc.* **224**, 801.
Kaler, J. B. (1966) *Astrophys. J.* **143**, 722.
Kaler, J. B. (1968) *Astrophys. Letters* **1**, 227.
Miller, J. S. (1971) *Astrophys. J. (Letters)* **165**, L101.
Nazarenko, A. F. (1990) *Astrofiz. Issled. (Isv. SAO)* **32**, 166.
Pottash, S. R. (1960) *Astrophys. J.* **131**, 202.
Salem, M. and Brocklehurst, M. (1979) *Astrophys. J. Suppl.* **39**, 633.
Sevastyanenko, V. (1985) *Beitr. Plasmaphys.* **25**, 151.
Sorochenko, R. L., Rydbeck, G. and Smirnov, G. T. (1988) *Astron. Astrophys.* **198**, 233.
Spitzer, L. (1968) *Diffuse Matter in Space* (J. Willey and Sons: New York).
Summers, H. P. (1977) *Mon. Not. R. Astr. Soc.* **178**, 101.
Wilson, T. L. and Pauls, T. A. (1984) *Astron. Astrophys.* **138**, 225.